Development of Prediction Model for Vortex-Induced Motion of Multi-Column Floating Structure

Conference Paper · June 2018

CITATIONS
0

READS
4

4 authors, including:

Hideyuki Suzuki
The University of Tokyo
106 PUBLICATIONS **288** CITATIONS
SEE PROFILE

Rodolfo Trentin Gonçalves
The University of Tokyo
93 PUBLICATIONS **453** CITATIONS
SEE PROFILE

Proceedings of the Twenty-eighth (2018) International Ocean and Polar Engineering Conference **www.isope.org**
Sapporo, Japan, June 10-15, 2018

ISBN 978-1-880653-87-6; ISSN 1098-6189

Development of Prediction Model for Vortex-Induced Motion of Multi-Column Floating Structure

Seiya Shiiba, Shinichiro Hirabayashi, Hideyuki Suzuki, Rodolfo Trentin Gonçalves

Department of Ocean Technology, Policy, and Environment
School of Frontier Sciences, The University of Tokyo
Kashiwa-no-ha, Kashiwa-shi, Chiba, Japan

ABSTRACT

A simple prediction model for VIM of multi-column floaters was developed. The model solved the one degree of freedom equation of motion which included inertia, damping, restoration and external force term. Inertia, damping and external force terms were obtained experimentally from measurements of forced oscillation tests with and without towing velocity (current incidence). The numerical model using the force coefficients from experiments was tested for an array with four circular cylinders in a square configuration with column spacing ratio (distance between column centers) equal to 2 and 3. The numerical results were compared with VIM experiments, and the estimated motion amplitude showed a good agreement. The numerical results were able to evaluate the influence of the spacing ratio for the array with four circular columns.

KEY WORDS: vortex-induced motion; forced oscillation and towing experiment; hydrodynamic force; low aspect ratio; added mass coefficient; damping coefficient.

INTRODUCTION

The Floating Offshore Wind Turbine (FOWT) presents complex motion because the wind turbine is subject to wind and the floater is subject to waves and currents. Moreover, in a current, the floating structure is known to present periodic motion excited by the pressure oscillation caused by the vortex shedding. This behavior is called Vortex-Induced Motion (VIM), which has a similar generation mechanism to the so-called Vortex-Induced Vibration (VIV). VIM may cause severe effects on the fatigue of the mooring system. From the viewpoint of cost reduction, it is desirable not to exchange mooring cables. However, the influence of VIM on floating structures has not been quantitatively estimated sufficiently.

Although the VIM and VIV generation mechanisms are the same, there are some different characteristics between them. While VIM occurs for a structure with small aspect ratio with oscillations as a rigid body, VIV occurs for a structure with large aspect ratio and vibrates with elastic deformation. Since a structure with low aspect ratio has a small draft, the effect of three-dimensional flow becomes stronger than that with high aspect ratio. VIM usually exhibits a long oscillation period as compared to VIV.

The VIM characteristic on the monocolumn floater (single circular cylinder) was investigated using a large model in supercritical Reynolds number (Re=1.5×10^5~7.0×10^5) by a towing experiment in Fujiwara *et al.* (2013). The VIM amplitude is was shown to be significantly different from the result of the small Reynolds number. Their results showed that the non-dimensional motion amplitude of the small model is larger than that of the large model in both in-line and cross-flow direction. They concluded that this is due to the unstable situation around the model affected by the Reynolds number.

Experiments regarding the FIM - flow-induced motion on an array of three and four floating cylinders with low aspect ratio were performed in Gonçalves *et al.* (2017, 2018a, 2018b). In these experiments, the FIM of an array of cylinders with various section geometries were measured in the towing tank. Significant effects of column geometry, arrangement, and spacing on the behavior of FIM for multi-column platforms can be found in these works.

The VIM motions and the hydrodynamic forces acting on each cylinder of a multi-column offshore floating structure were investigated by Hashiura *et al.* (2016). Their results showed that the total hydrodynamic force is more significant for the smaller distance between column centers, $L/D = 3$. Also, the transverse force amplitude of the front cylinder becomes large compared to that of the rear cylinder.

Some numerical evaluations of VIM for single cylinder were conducted by Rosetti *et al.* (2012). In this numerical model, a phenomenological model was applied to solve the van der Pol equations. Good agreements between numerical simulations and experiments were presented.

In the previous research, it is possible to find experimental studies on VIM of multi-column platforms, but it was not possible to find numerical studies, except for CFD calculation for predicting the VIM behavior of this kind of platforms.

We here aimed to develop a simple numerical model to predict the VIM of a multi-column floating structure using the hydrodynamic model, which is adapted for the practical VIV behavior analysis method based on the works by Sarpkaya (1978) and Gopalkrishan (1993). The technique developed by Sarpkaya (1978) and followed by Gopalkrishan (1993) modeled the hydrodynamic force from the experimental data obtained from forced oscillation and a towing experiment.

To obtain the hydrodynamic force data for a multi-column floating structure, towing experiments with forced oscillation were conducted, following the methodology by Gopalkrishan (1993). The hydrodynamic force data was summarized as a function of oscillating frequency and amplitude. An oscillation estimation filter that estimates the current oscillation state was used. The validity of this prediction model was verified by comparing with the results with those of previous studies.

NUMERICAL MODEL

Outline of the VIM prediction model

The equation of motion for one degree of freedom of the floating body can be expressed by the following equation.

$$\mathrm{M}(1+C_{add})\ddot{y}+C_{U\_damp}\dot{y}+ky=F_V\sin(\omega_{vortex}t+\theta) \quad (1)$$

where M is the mass of the system; $C_{add}$is the added mass coefficient; C_{U_damp} is the damping coefficient; k is the restoring constant; F_V is the lift force due to the vortex shedding; ω_{vortex} is the vortex shedding angular frequency; ρ is the fluid density; D is the cylinder diameter; U is the towing velocity.

The calculation procedure of the VIM prediction model is as follows. A flowchart of the VIM prediction model is shown in Fig.1.

1. Read the hydrodynamic force from experiments, which is a function of amplitude and frequency.
2. Set the initial value of the position, velocity and external force of the body.
3. Solve the equation of motion by Eq. 1.
4. Record the histories of displacement estimating the oscillation state.
5. Estimate the oscillation frequency and amplitude from the recent histories of displacement using the oscillation estimation filter.
6. Decide the hydrodynamic force, which is a function of oscillation frequency and amplitude.
7. Repeat procedures 1 ~ 6 iteratively.

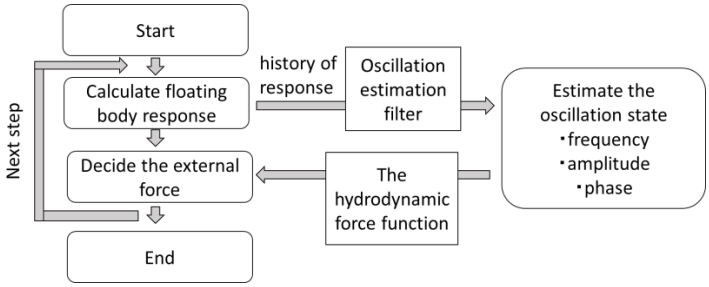

Fig.1 Flowchart of the VIM prediction model

For solving the motion equation, a 4th order Runge-Kutta method was used. The wave radiation damping is not considered in this paper.

The oscillation estimation filter

The oscillation estimation filter estimates the recent frequency and amplitude of oscillation from the past displacement history. This filter is based on the method by Tejima (2006) using discrete Fourier transform. The equation of the oscillation estimation filter is expressed by the following equations.

$$a_i=\beta\int_{t-NT_i}^{t}y(\tau)\sin(2\pi f_i\tau)e^{-\alpha(t-\tau)}d\tau \quad (2)$$

$$b_i=\beta\int_{t-NT_i}^{t}y(\tau)\cos(2\pi f_i\tau)e^{-\alpha(t-\tau)}d\tau \quad (3)$$

$$\alpha=-\ln\left(\frac{X}{100}\right)\frac{f_i}{N} \quad (4)$$

$$\beta=\frac{2\alpha}{1-e^{-\frac{\alpha N}{f_i}}} \quad (5)$$

$$A_i=\sqrt{a_i^2+b_i^2} \quad (6)$$

where α is a weighting function for time, and β is a correction factor; N is the number of waves to be used in the oscillation estimation; A_i is calculated for various frequencies f_i, and frequency f_i with the maximum value of A_i was chosen for the oscillation frequency at that time. In this research, to capture the transient response in which the oscillation develops, N is set to 2 waves. Unstable fluctuations were suppressed by applying the moving average for estimated frequency and amplitude.

The hydrodynamic force coefficients

The hydrodynamic force coefficients were obtained from the measurement data by the following procedure. The oscillation of the floating system is expressed by the flowing equation.

$$\mathrm{y(t)}=A_0\sin(\omega t) \quad (7)$$

Considering that the hydrodynamic forces have the same frequency as the motion oscillation, the following equation can be written:

$$\begin{aligned}F_H(t)&=F_H(y)sin(\omega t+\varphi)\\&=F_H(y)[sin(\omega t)cos(\varphi)+cos(\omega t)sin(\varphi)]\end{aligned} \quad (8)$$

This force can be decomposed into a component proportional to the acceleration, F_{Add}, and a component proportional to the velocity, F_{Damp}, using orthogonality of trigonometric functions as depicted in Fig.2. Each component was non-dimensionalized by the following equations.

$$C_{damp}=\frac{F_{Damp}}{\frac{1}{2}\rho DLUA(2\pi f)} \quad (9)$$

$$C_{add}=\frac{F_{Add}-MA(2\pi f)^2}{\frac{1}{2}\rho DLUA(2\pi f)} \quad (10)$$

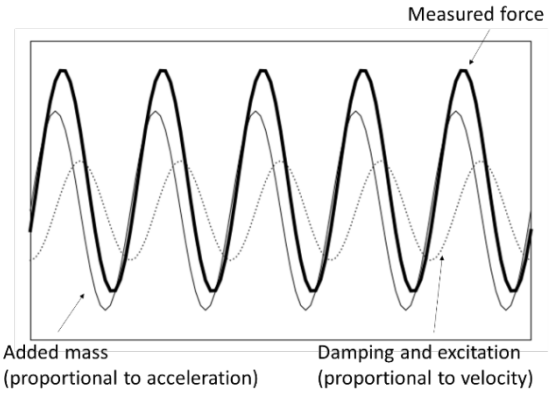

Fig.2 Decomposition of the hydrodynamic force

where C_{damp} and C_{add} correspond to damping and added mass coefficients. F_{damp} is the hydrodynamic force component proportional to the velocity of the system; F_{add} is the hydrodynamic force component proportional to the acceleration of the system; ρ is a fluid density. The hydrodynamic force coefficients were functionalized by the linear interpolation of the database concerning $f_{osc}D/U$ and A_{osc}/D. The hydrodynamic coefficients were determined when the system was in steady state, which will be shown in the analysis section.

EXPERIMENTAL DETAILS

The towing experiments with forced oscillation were conducted in the towing tank at The University of Tokyo, Japan. The dimensions of the tank are 85m in length × 3.5m in width × 2.5m in height.

In these experiments, four circular cylinders were arranged in a square array configuration. Each cylinder was fixed with each other above the water surface by metallic bars. The floaters were fixed to the forced oscillator by a spacer, which was used to adjust the draft. The experimental schematic is shown in Fig.3~4. The cylinder models were made of acrylic.

The main parameters of the test configurations are shown in Table 1. The column distances, S/D, were 2.0 and 3.0. Nineteen cases of the oscillation frequency, f_{osc}, were performed as well as nine cases of oscillation amplitude, A_{osc}. The oscillation direction was the cross-flow direction.

The amplitude range of the experiments comprised the response amplitudes observed in the FIM studies tests by Gonçalves *et al.* (2017, 2018a). The authors showed maximum response amplitudes in the transverse direction around 1.0D for the array with four circular cylinders. The imposed amplitudes of the present work were limited to 0.8 D because of the apparatus setup. The towing velocity was set to 0.3 m/s, which corresponds to Re = 75,000. This is within the range of the conditions of the comparative study by Gonçalves *et al.* (2017, 2018a), and we believe that the effect of Re is not significant in this subcritical range. Forces were measured at each cylinder separately using three-dimensional load cells with a capacity of 100N. The sampling frequency was 100 Hz. The experimental cases are shown as black points in the graphs presented in Fig.5~6.

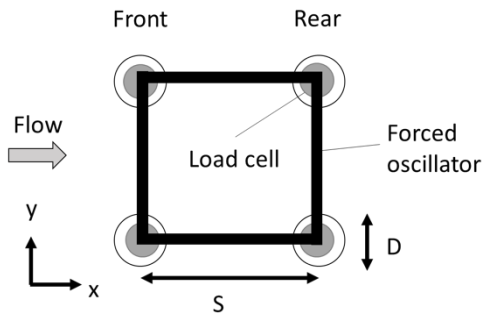

Fig.3 Top view of four circular cylinders arrangements

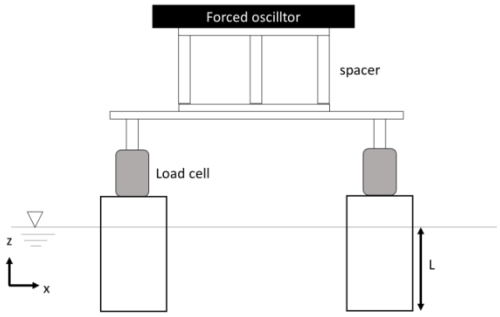

Fig.4 Side view of four cylindrical arrangements

Table 1 Main parameters

Parameter	Symbol	Value	Unit
Cylinder diameter	D	0.25	m
Mass of floating system	M	44	kg
Towing speed	U	0.3	m/s
Oscillation amplitude	Aosc/D	0.1-0.8	-
Oscillation frequency	foscD/U	0.05-0.35	-
Aspect ratio	L/D	1.5	-
Column distance	S/D	2.0,3.0	-
Reynolds number	Re	75,000	-

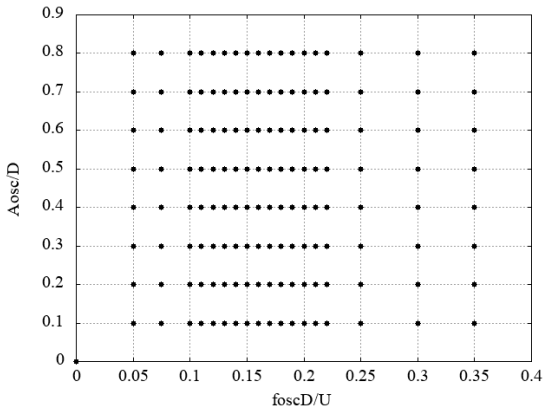

Fig.5 Experimental cases (S/D=3.0)

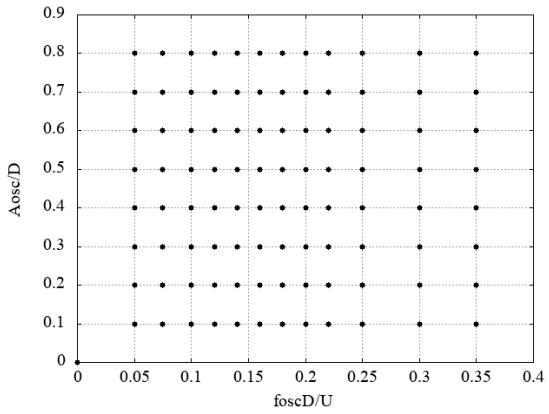

Fig.6 Experimental cases (S/D=2.0)

EXPERIMENTAL RESULTS FROM TOWING AND FORCED OSCILLATIONS

The results from the towing experiment with forced oscillation are shown in Fig.7~14. Fig.7~10 show the force coefficient results for the column distance $S/D = 3.0$, and Fig.11~14 show the force coefficient results of the column distance $S/D = 2.0$.

The results showed that the added mass coefficient was the maximum for $f_{osc}D/U = 0.15$ in Fig.9 and 10. Also, the damping coefficient is verified to take a negative value for $f_{osc}D/U = 0.10$ to 0.15 in Fig.9~10. These results are considered to be the influence of excitation force due to vortex shedding. As the oscillation amplitude increased, the value of $f_{osc}D/U$ for the peak of the excitation force decreased. This result means that when the amplitude increased to an absolute limit, the negative damping force disappeared and the oscillation stabilized.

Moreover, it can be confirmed that the added mass coefficient is a negative value when $f_{osc}D/U$ is low, as in Fig.7, 8 and 11. This result is consistent with the findings shown by Sarpkaya (2004) and Vikestad *et al.* (2000). Sarpkaya (2004) discussed the results of the towing experiment of a single cylinder with forced oscillation in the cross-flow direction. The results showed that when the ratio of the frequency of oscillation of a body to the vortex shedding frequency is small, the added mass coefficient becomes the negative value, and when the ratio exceeds 0.85, the added mass coefficient becomes a positive value. This behavior is because if the ratio exceeds 1, the phase of the fluid force changes from the phase opposite to the displacement of the floating body to the same phase.

For $S/D = 2.0$, there were significant differences when comparing the results for $S/D = 2.0$ and $S/D = 3.0$.The added mass coefficient of the front column for $S/D = 2.0$, as in Fig.10, showed a similar tendency to that of the front column with $S/D = 3.0$, but the results of the rear column, as in Fig.12, were entirely different. The added mass coefficient of the rear column decreased to nearly $f_{osc}D/U = 0.15$. Also, the largest added mass coefficient value occurred between $f_{osc}D/U = 0.15$ to 0.10.

An impressive result was obtained for the damping coefficient for $S/D = 2.0$. In Fig.13 and 14, when $f_{osc}D/U = 0.10$ to 0.15, the negative damping force acted on the front column, while the positive damping force acted on the rear column. On the other hand, when $f_{osc}D/U = 0.15$ to 0.20, the damping force acted on the front column, but the excitation force acted on the rear column. This result showed that the oscillation in the transverse direction of the floating body does not develop, but the yaw motion is excited.

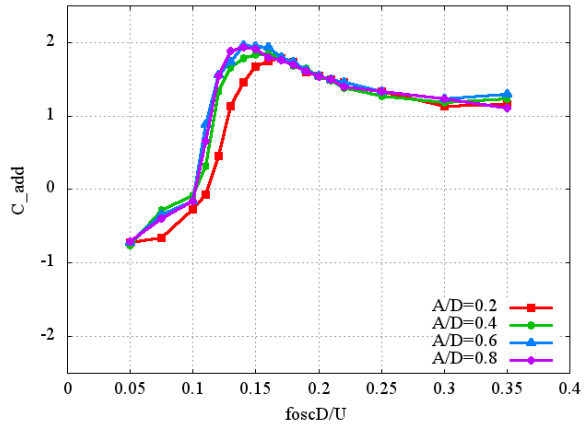

Fig.7 Mean added mass coefficient of the front column at S/D=3.0

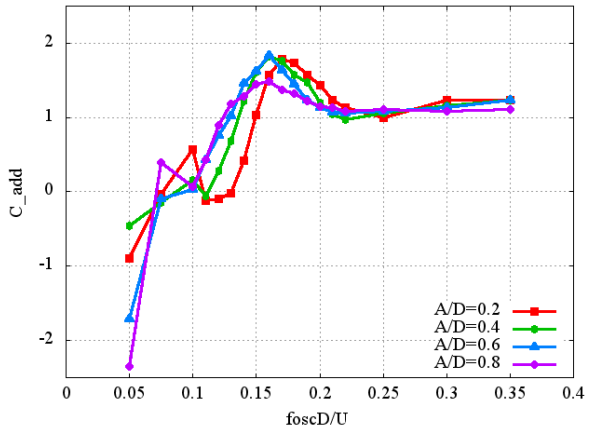

Fig.8 Mean added mass coefficient of the rear column at S/D=3.0

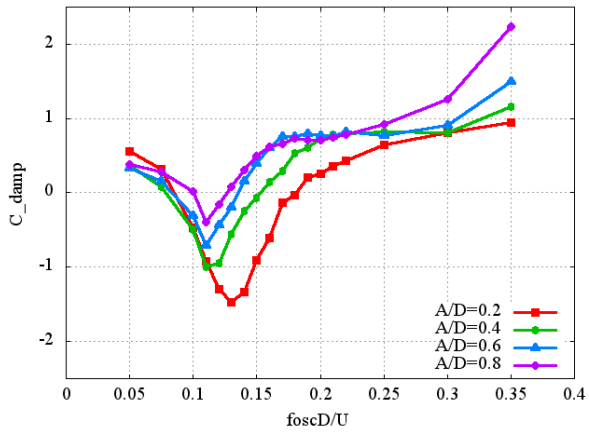

Fig.9 Mean damping coefficient of the front column at S/D=3.0

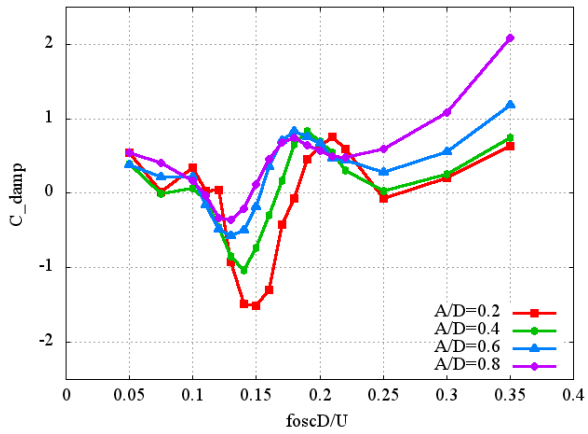

Fig.10 Mean damping coefficient of the rear column at S/D=3.0

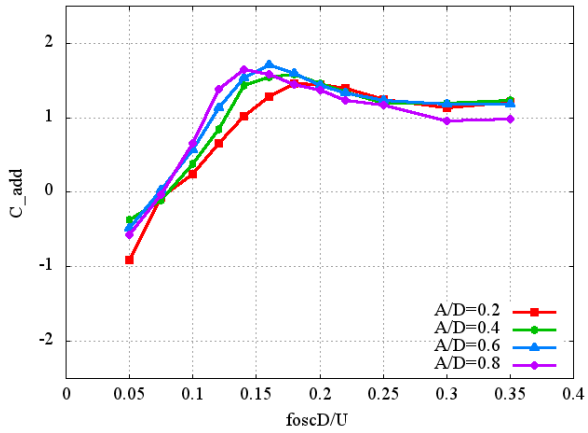

Fig.11 Mean added mass coefficient of the front column at S/D=2.0

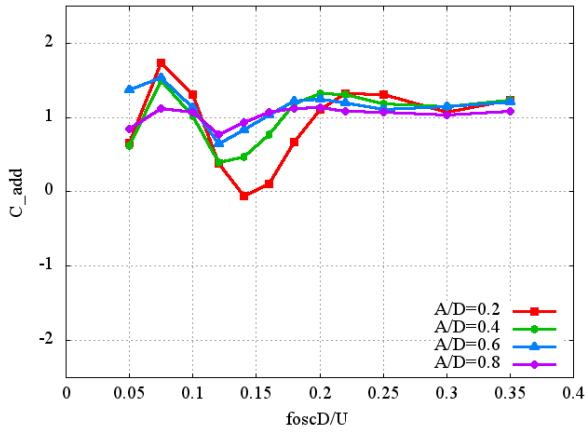

Fig.12 Mean added mass coefficient of the rear column at S/D=2.0

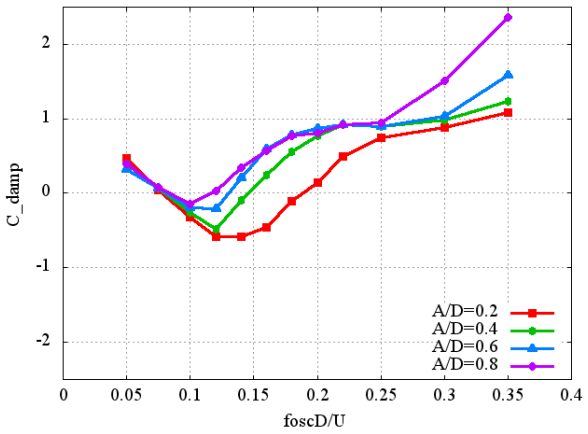

Fig.13 Mean damping coefficient of the front column at S/D=2.0

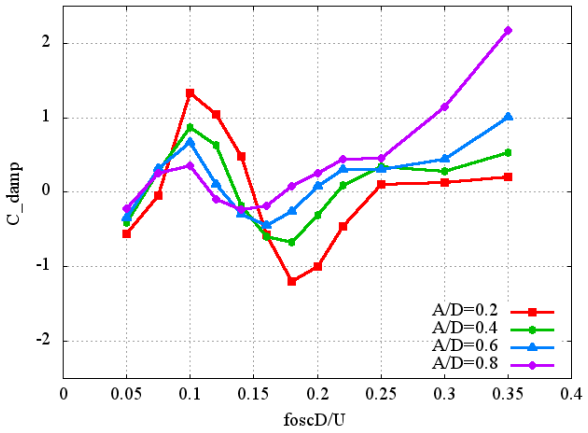

Fig.14 Mean damping coefficient of the rear column at S/D=2.0

VIM PREDICTION RESULTS

To verify the validity of the results from the VIM prediction program, the nominal displacement of the VIM tests of the 4-column floating body by Gonçalves *et al.* (2018a) were used for comparison. Table 2 summarizes the parameters used for calculating the VIM amplitude. The added mass and the damping coefficients were obtained by linear interpolation in the region inside the measurement conditions and cubic spline extrapolation in the region outside the measurement conditions. Also, when the excitation frequency was low, the frequency component of the vortex shedding was confirmed separately from the excitation frequency. However, when the excitation frequency exceeded 0.11, the synchronization of the vortex emission frequency and the excitation frequency was confirmed. Therefore, until the excitation frequency of the floating body exceeds 0.11, the lift force due to the vortex shedding was given as an external force.

The nominal VIM amplitude for each column-to-column distance calculated by the VIM prediction model and the experimental results by Gonçalves *et al.* (2018a) are shown in Fig. 15.

Table 2 Calculation conditions

Parameter	Symbol	Value	Unit
Diameter	D	0.25	m
Towing speed	U	0.3	m/s
Restoring constant	k	84-930	-
Aspect ratio	L/D	1.5	-
Column distance	S/D	2.0,3.0	-
Reynolds number	Re	75,000	-

As can be seen in Fig. 15, the results from the numerical prediction and the experiments showed a good agreement for the range of $4 < V_r < 6$. On the other hand, the extrapolation of the hydrodynamic force coefficients for the larger reduced velocities was a source of increasing differences.

In the range of $V_r > 8$, it was confirmed that the VIM amplitude of $S/D = 2$ calculated by the VIM prediction model remarkably decreased. This behavior could indicate the end of the synchronization between the motion and the vortex shedding. However, there is a large difference between prediction and experiment in this range. This discrepancy may also be the result of the extrapolation of missing hydrodynamic force coefficients in large amplitude.

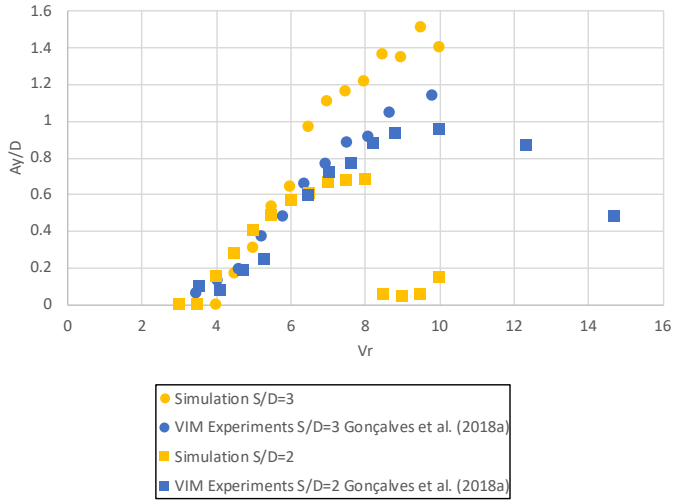

Fig.15 Comparison of the predicted and experimented VIM amplitudes.

CONCLUSIONS

The hydrodynamic forces on the VIM phenomenon were investigated by the towing experiment with forced oscillation. The added mass coefficient and damping coefficient were obtained from the measurement of the hydrodynamic force.

The damping coefficient of both front and rear column with $S/D = 3.0$ was a negative value for $f_{osc}D/U = 0.10$ up to 0.15. This behavior derived from the influence of the excitation forces due to vortex shedding.
It was confirmed that the added mass coefficient became negative when the oscillation frequency was low.

Different results were obtained for different spacing ratios for the added mass coefficient. This behavior was because of the influence of vortex interference and inter-column interference due to the change in column distance.

The transient response of VIM was reproduced using hydrodynamic force function. Within the conditions under which the forced oscillation experiment was carried out, the calculation result using the VIM prediction model agreed well with the previous experiment result. If more forced oscillation experiments are carried out, further improvement in accuracy is expected.

This work can be a valuable database for future calculations using the VIM prediction model.

REFERENCES

Fujiwara, T, Nimura, T, Shimozato, K, and Matsui, R (2016) "VIM model test and assessment on a semi-submersible type floater with different column intervals," *Proc of the ASME 35th International Conference on Ocean, Offshore and Arctic Engineering*, OMAE2016-54308, Busan, South Korea.

Gonçalves, RT, Chame, MEF, Hannes, NH, Lopes, PPSP, Suzuki, H, and Hirabayashi, S. (2017) "Experimental flow-induced motions of array of floating cylinders with circular, square and diamond sections," *Proc of the 24th ABCM International Congress of Mechanical Engineering*, COBEM-2017-0441, Curitiba, PR, Brazil.

Gonçalves, RT, Hannes, NH, Chame, MEF, Lopes, PPSP, Marques, MA, Hirabayashi, S, and Suzuki, H (2018a) "Experimental study on flow-induced motion of an array of four cylinders with different spacing ratio," *Proc of the OCEANS'18 MTS/IEEE Kobe, Techno-Ocean 2018 (OTO' 18),* Kobe, Japan.

Gonçalves, RT, Chame, MEF, Hannes, NH, Lopes, PPSP, Hirabayashi, S, and Suzuki, H (2018b) "Experimental study on flow-induced motion of an array of three cylinders with circular, square, and diamond sections," *Proc of the 28th International Ocean and Polar Engineering Conference*, Sapporo, Hokkaido, Japan.

Gopalkrishan, R (1993) "Vortex-Induced Forces on Oscillating Bluff Cylinders," *D.Sc. Thesis*, Department of Ocean Engineering, MIT, Cambridge, USA.

Hashiura, M, Hirabayashi, S, and Suzuki, H (2016) "Experimental study of shape effect of floating body for Vortex-Induced Motion," *Proc of the Techno-Ocean 2016*, Kobe, Japan.

Rosetti, GF, Gonçalves, RT, Fujarra, ALC, and Nishimoto, K (2011) "Parametric Analysis of a Phenomenological Model for Vortex-Induced Motions of Monocolumn Platforms," *J. of the Braz. Soc. of Mech. Sci. & Eng.*, Vol. 33, pp. 139-146.

Tejima, T, Suzuki, H, and Sato, T (2006) "Time Evolution of VIV Response of Towed Pipe Based on Hydrodynamic Force Chart Calculated by CFD", *J. Jpn. Inst. Marine Engrg.*, Vol. 41, No.2, pp.152-157 (in Japanese).

Sarpkaya, T (1978) "Fluid forces on oscillating cylinders", *Journal of Waterway port Coastal and ocean Division ASCE*, Vol. 104, pp. 275-290.

Sarpkaya, T (2004) "A critical review of the intrinsic nature of vortex-induced vibrations", *Journal of Fluids and Structures*, Vol. 19(4), pp. 389–447.

Vikestad, K, Vandiver, JK, and Larsen, CM (2000) "Added mass and oscillation frequency for a circular cylinder subjected to vortex-induced vibration and external disturbance," *Journal of Fluids and Structures*, Vol. 15, pp. 1031–1060.